American Mineralogist, Volume 76, pages 1–7, 1991

Crystal structures of $Mg_{12}Si_4O_{19}(OH)_2$ (phase B) and $Mg_{14}Si_5O_{24}$ (phase AnhB)

Larry W. Finger, Robert M. Hazen, Charles T. Prewitt
Geophysical Laboratory, Carnegie Institution of Washington, Washington, DC 20015, U.S.A.

Abstract

The crystal structures of two high-pressure magnesium silicates with mixed four- and six-coordinated Si have been solved and refined. The crystals were synthesized in the split-sphere, cubic anvil apparatus (USSA-2000) located at the Stony Brook High-Pressure Laboratory. Phase B, $Mg_{12}Si_4O_{19}(OH)_2$, crystallizes in space group $P2_1/c$ with 40 atoms in the asymmetric unit. Phase AnhB, $Mg_{14}Si_5O_{24}$, occurs in space group *Pmcb* with 18 atoms per asymmetric unit. Final values of the standard *R*-factors were 0.056 and 0.029 for the observed reflections of phases B and AnhB, respectively. Both structures contain two types of layers, one with edge-shared Mg and Si octahedra, and the other with Mg octahedra and Si tetrahedra and the stoichiometry of humite for phase B, and forsterite for phase AnhB. Each octahedral layer is flanked by two of the tetrahedral layers, with a total of six layers per unit cell. Each Si octahedron shares all 12 edges with Mg octahedra, forming a cluster with 13 octahedral cations. This dense packing contributes to the relatively high zero-pressure densities of 3.368 and 3.435 g cm^{-3} for phases B and AnhB, respectively. This study also demonstrates that high-pressure materials do not always have simple structures.

Introduction

The H_2O content of the mantle has a critical effect on its melting relations and seismic properties. As a consequence, potential minerals for storage of H and/or H_2O in the mantle have been the subject of considerable speculation and experimentation. In addition to normal hydrous magnesium silicates, a number of potential phases are shown in Table 1, including the 10-Å phase (Sclar et al., 1965), phases A, B, and C (Ringwood and Major, 1967), norbergite and humite (Ribbe, 1980), chondrodite or phase D (Yamamoto and Akimoto, 1977), clinohumite (McGetchin et al., 1970; Yamamoto and Akimoto, 1977), β-Mg_2SiO_4 (Smyth, 1987; Downs, 1989), phase E (Kanzaki, 1989; Kudoh et al., in preparation), the 3.65-Å phase (Rice et al., 1989), and superhydrous B (Gasparik, 1990). Although none of these phases can be eliminated from consideration, some of them seem to be less likely than others to be important in the mantle. For example, if β-Mg_2SiO_4 contains H, there must be an associated charge-compensating defect such as a Mg vacancy (Smyth, 1987). At high pressures, it does not seem likely that this process would lead to the storage of much H. Several of the other phases have densities and upper pressure stabilities that are too low for mantle phases. The 10-Å phase has a zero-pressure density of 2.65 g cm^{-3} with a maximum synthesis pressure of 9 GPa (Sclar et al., 1965; Sclar and Carrison, 1966). The densities of phases A (Horiuchi et al., 1979) and B (Akaogi and Akimoto, 1980) are 2.96 and 3.32 g cm^{-3}, respectively. Phase E has a low density (2.8 g cm^{-3}); furthermore, it is probably metastable and might not be present under Earth conditions.

Because of the availability of suitable crystals of phase B and its possible importance in H_2O storage in the mantle, this study was undertaken. The present report will discuss details of the crystallographic and crystal chemistry relations of phases B and AnhB, a related anhydrous magnesium silicate. Finger et al. (1989) presented a discussion of the petrologic significance of the crystal chemistry of these phases. Finger and Prewitt (1989) used the crystal chemical features of these phases to predict potential compositions for other high-density hydrous phases.

Experimental

Crystals of phase B, synthesized at 1200 °C and 12 GPa in the split-sphere, cubic anvil apparatus (USSA-2000), were obtained from the Stony Brook High-Pressure Laboratory. Selected crystals displayed sharp diffraction patterns with no diffuse scattering for either TEM or X-ray photographs; however, some crystals demonstrate pseudomerohedral twinning by a twofold operator parallel to [001]. A crystal with dimensions 0.06 × 0.12 × 0.17 mm was mounted on a Rigaku AFC-5R four-circle diffractometer operated at 45 kV, 180 ma. The intensities in a hemisphere of reciprocal space with $\sin\theta/\lambda \leq 0.70$ were measured using Mo radiation and a graphite monochromator. The resulting intensities were corrected for absorption and Lorentz-polarization effects using a modified version of the program of Burnham (1966). Transmission factors ranged from 0.87 to 0.94. The resulting structure factors were averaged in Laue group $2/m$ to yield an independent set of 4263 structure factors (Ta-

0003–004X/91/0102–0001$02.00

TABLE 1. Hydrous magnesium silicates

Phase	Composition	Fraction 6 coordination Si	Density (g cm^{-3})	Reference
Serpentine	$Mg_3Si_2O_5H_4$	0.00	2.55	Deer et al. (1962)
Talc	$Mg_3Si_4O_{12}H_2$	0.00	2.79	Deer et al. (1962)
Anthophyllite	$Mg_7Si_8O_{24}H_2$	0.00	3.01	Deer et al. (1963)
Norbergite	$Mg_3SiO_6H_2$	0.00	?	Ribbe (1980)
Chondrodite or phase D	$Mg_5Si_2O_{10}H_2$	0.00	3.06	Yamamoto and Akimoto (1977)
Humite	$Mg_7Si_3O_{14}H_2$	0.00	?	Ribbe (1980)
Clinohumite	$Mg_9Si_4O_{18}H_2$	0.00	3.14	Yamamoto and Akimoto (1977)
Phase A	$Mg_7Si_2O_{14}H_6$	0.00	2.96	Horiuchi et al. (1979)
Phase B	$Mg_{12}Si_4O_{21}H_2$	0.25	3.37	This study
Phase C	?	?	?	Ringwood and Major (1967)
Phase E	$Mg_{2.17}Si_{1.01}O_6H_{3.62}$	0.00	2.78	Kudoh et al. (in preparation)
Phase E	$Mg_{2.08}Si_{1.16}O_6H_{3.20}$	0.00	2.88	Kudoh et al. (in preparation)
10 Å	$Mg_3Si_4O_{14}H_6$	?	?	Yamamoto and Akimoto (1977)
3.65 Å	$Mg_{1.4}Si_{1.3}O_8H_8$	?	?	Rice et al. (1989)
Superhydrous B	$Mg_{10}Si_3O_{18}H_4$	0.33(?)	?	Gasparik (1990)

ble 2).[1] Of these, 3254 have $I > 2\sigma_I$. The internal agreement in the symmetry averaging was 3.5%. The extinction symbol is $P12_1/c1$, which leads to $P2_1/c$ as the space group. Structure solution was attempted with program Mithril (Gilmore, 1984); however, there was little success. The most likely explanation for this failure is the pseudosymmetry of the O substructure, which has essentially a cubic-closest-packing arrangement.

While the structure solution for phase B was being undertaken, a new phase, described by Herzberg and Gasparik (1989), synthesized at 2380 °C and 16.5 GPa from a charge dried in Ar, became available. Electron probe analyses of this material yielded an atomic Mg/Si ratio of 2.81 and a total analysis close to 100%; therefore, the new phase was believed to be anhydrous. A crystal with dimensions 0.03 × 0.18 × 0.21 mm was mounted on the diffractometer and the intensity data were measured and processed as described above. Transmission factors ranged from 0.81 to 0.92, and there were a total of 1337 independent structure factors in Laue group *mmm*. Of these, 1132 have $I > 2\sigma_I$. The internal agreement for the structure factor average is 2.5%. The extinction symbol is *P-cb*, yielding *P2cb* or *Pmcb* as the possible space groups. The latter choice is employed in all computations. This structure also has pseudosymmetry in the O substructure; however, it has a Si atom at the origin. As a result, the direct-methods program yielded an *E*-map that could be interpreted. Fourier syntheses from the partial structure resulted in a complete solution. Crystal structure refinement with anisotropic temperature factors, neutral scattering factors, and anomalous scattering coefficients was completed with program RFINE90, a development version of program RFINE4 (Finger and Prince, 1975). Table 3 lists the atomic coordinates, equivalent isotropic temperature factors, and valence sums (Brown, 1981) for the anhydrous phase. Valence sums for O ions are consistent with the hypothesis that no H is present. After completion of the solution of the structure, the description of an isostructural germanate (Von Dreele et al., 1970) was discovered.

When the crystal structure of phase AnhB was compared with the partial structures for phase B, it seemed likely that the choice of origin was a complicating factor. To remove this difficulty, further calculations were performed in space group *Pc*. This choice proved beneficial

TABLE 3. Crystallographic data for $^{[6]}Mg_{14}{}^{[6]}Si^{[4]}Si_4O_{24}$ (phase AnhB)

Atom	*x*	*y*	*z*	B_{eq}	VS*
Si1	0	0	0	0.33(2)**	3.7
Si2	½	0.31141(5)	0.17445(7)	0.35(1)	4.1
Si3	0	0.37524(5)	0.99754(8)	0.34(1)	3.7
Mg1	½	0	½	0.47(2)	2.0
Mg2	½	0.17460(6)	0.35469(9)	0.46(1)	2.0
Mg3	½	0	0	0.48(2)	1.9
Mg4	0.24050(9)	0.00241(4)	0.25354(6)	0.44(1)	2.1
Mg5	0	0.17612(6)	0.82058(9)	0.48(1)	2.0
Mg6	0.24396(10)	0.16958(4)	0.08108(6)	0.46(1)	2.0
O1	0	0.91394(13)	0.34705(18)	0.47(3)	1.9
O2	0	0.57564(12)	0.35375(19)	0.37(3)	2.1
O3	0	0.24165(12)	0.49605(19)	0.45(3)	1.9
O4	½	0.08599(13)	0.17186(18)	0.44(3)	1.9
O5	½	0.42488(12)	0.16958(19)	0.42(3)	2.3
O6	½	0.76001(13)	0.47153(16)	0.44(3)	2.2
O7	0.2342(2)	0.08741(8)	0.42136(11)	0.45(2)	1.9
O8	0.2147(2)	0.42653(8)	0.42534(12)	0.47(2)	1.9
O9	0.2824(2)	0.76221(8)	0.25276(12)	0.48(2)	2.1

Note: Diffraction experiments with Rigaku AFC-5 diffractometer, rotating anode generator, Mo$K\alpha_1$ radiation, graphite monochromator, $\lambda = 0.7093$ Å, ω step scans, ambient pressure and temperature. $a = 5.868(1)$ Å; $b = 14.178(1)$ Å; $c = 10.048(1)$ Å; $V_{cell} = 835.9$ Å^3. Space group *Pmcb*; $Z = 2$; molecular mass = 864.8 g; $\rho_{calc} = 3.435$ g cm^{-3}; $\mu_l = 10.8$ cm^{-1}. $R = \Sigma||F_o| - |F_c||/\Sigma|F_o| = 0.040$, $R_w = \Sigma w_F(F_o - F_c)^2/\Sigma w_F F_o^2 = 0.024$ for all 1337 independent data; $R = 0.029$, $R_w = 0.024$ for 1132 data with $F_o > 2\sigma_F$; goodness of fit = 0.9 for anisotropic temperature factors; $w_F = [\sigma_F + (0.015F)^2]^{-2}$. Largest shift/error in final cycle is 0.23.

* VS is valence sum of Brown (1981).

** Numbers in parentheses are the estimated standard deviations in the last quoted decimal place. This convention is followed in all subsequent tables.

[1] A copy of the observed and calculated structure factors and standard deviations for both phases (Table 2) may be ordered as Document AM-91-451 from the Business Office, Mineralogical Society of America, 1130 Seventeenth Street NW, Suite 330, Washington, DC 20036, U.S.A. Please remit $5.00 in advance for the microfiche.

TABLE 4. Crystallographic data for $^{[6]}Mg_{12}{}^{[6]}Si^{[4]}Si_3O_{19}OH)_2$ (phase B)

Atom	x	y	z	B_{eq}	VS*
Si1	0.79007(9)	0.00099(8)	0.07415(10)	0.24(1)	3.6
Si2	0.49753(9)	0.18964(7)	0.67358(10)	0.35(2)	4.1
Si3	0.21336(10)	0.12550(7)	0.42675(10)	0.30(2)	3.7
Si4	0.78120(10)	0.12333(7)	0.57300(10)	0.31(2)	3.8
Mg1	½	0	½	0.56(3)	2.1
Mg2	0.49776(11)	0.17451(9)	0.35639(12)	0.45(2)	2.1
Mg3	½	0	0	0.50(3)	1.8
Mg4	0.65272(11)	0.00249(12)	0.29314(10)	0.47(2)	2.0
Mg5	0.07515(11)	0.00035(10)	0.15240(11)	0.42(2)	2.0
Mg6	0.06509(11)	0.00035(10)	0.63472(12)	0.43(2)	1.9
Mg7	0.35160(11)	0.00277(10)	0.21545(12)	0.45(2)	2.1
Mg8	0.64927(11)	0.16994(9)	0.12361(12)	0.46(2)	2.0
Mg9	0.07005(11)	0.17303(9)	0.96971(12)	0.48(2)	2.0
Mg10	0.21857(11)	0.17720(9)	0.75197(11)	0.44(2)	2.0
Mg11	0.77446(11)	0.17593(9)	0.89486(12)	0.44(2)	2.1
Mg12	0.35095(11)	0.16857(9)	0.04510(12)	0.47(2)	2.0
Mg13	0.93431(11)	0.17750(9)	0.19882(12)	0.47(2)	2.1
O1	0.4984(2)	0.0752(2)	0.6696(2)	0.41(4)	2.2
O2	0.6474(2)	0.0869(2)	0.4613(2)	0.45(4)	1.9
O3	0.7832(2)	0.2400(2)	0.5726(2)	0.48(4)	2.1
O4	0.7830(2)	0.0858(2)	0.7289(2)	0.48(4)	2.0
O5	0.2152(2)	0.2425(2)	0.4249(2)	0.44(4)	2.0
O6	0.3472(2)	0.0875(2)	0.3842(2)	0.44(4)	1.9
O7	0.2104(2)	0.0871(2)	0.5816(2)	0.42(4)	2.0
O8	0.0806(2)	0.0881(2)	0.3171(2)	0.50(4)	2.0
O9	0.4989(2)	0.2413(2)	0.5293(2)	0.43(4)	2.2
O10	0.6203(2)	0.2386(2)	0.7795(2)	0.55(4)	2.1
O11	0.5002(2)	0.0851(2)	0.1721(2)	0.48(4)	1.8
O12	0.6667(2)	0.0744(2)	0.9698(2)	0.38(4)	1.9
O13	0.7928(2)	0.0757(2)	0.2192(2)	0.45(4)	2.0
O14	0.0863(2)	0.0714(2)	0.8220(2)	0.43(4)	2.0
O15	0.9182(2)	0.0796(2)	0.0279(2)	0.40(4)	1.8
O16	0.3331(2)	0.0734(2)	0.8838(2)	0.41(4)	1.9
O17	0.2088(2)	0.0729(2)	0.0711(2)	0.38(4)	2.0
O18	0.3748(2)	0.2392(2)	0.7155(2)	0.52(4)	2.1
O19	0.9116(2)	0.0852(2)	0.5285(2)	0.54(4)	1.6
O20	0.0675(2)	0.2477(2)	0.6369(2)	0.56(4)	1.3
O21	0.9218(2)	0.2481(2)	0.3639(2)	0.55(4)	1.3
H1	0.025(5)	0.193(4)	0.600(5)	1.7(12)	
H2	0.918(5)	0.204(4)	0.416(5)	1.2(13)	

Note: Diffraction experiments with Rigaku AFC-5 diffractometer, rotating anode generator, Mo$K\alpha_1$ radiation, graphite monochromator, $\lambda = 0.7093$ Å, ω step scans, ambient pressure and temperature. $a = 10.588(2)$ Å; $b = 14.097(1)$ Å; $c = 10.073(1)$ Å; $\beta = 104.10(3)°$; $V_{cell} = 1458.4(3)$ Å^3. Space group $P2_1/c$; $Z = 4$; molecular mass = 742.1 g; $\rho_{calc} = 3.368$ g cm^{-3}; $\mu_l = 10.3$ cm^{-1}. $R = \Sigma||F_o| - |F_c||/\Sigma|F_o| = 0.080$, $R_w = \Sigma w_F(F_o - F_c)^2/\Sigma w_F F_o^2 = 0.041$ for all 4263 independent data; $R = 0.056$, $R_w = 0.039$ for 3254 data with $F_o > 2\sigma_F$; goodness of fit = 1.0 for anisotropic temperature factors; $w_F = [\sigma_F + (0.015F)^2]^{-2}$; largest shift/error in final cycle is 0.43.

* VS is valence sum of Brown (1981). H bond contributions are not included.

and all non-H atoms were located and the R factor was reduced below 10%. The presence of a center of symmetry was verified and the space group was confirmed as $P2_1/c$. The final step was to locate the H atoms using the valence sums of Brown (1981). These values were within 0.2 units of the number expected for an O^{2-} except for O19, O20, and O21, which had values of 1.6, 1.2, and 1.3, respectively. It was possible to place two H atoms in OH-O bonding configurations such that all O atoms had valence sums on the order of 2. The trial H positions and isotropic thermal parameters were refined, along with anisotropic temperature factors for the remainder of the atoms. Table 4 lists the positions, equivalent isotropic temperature factors, and valence sums for phase B.

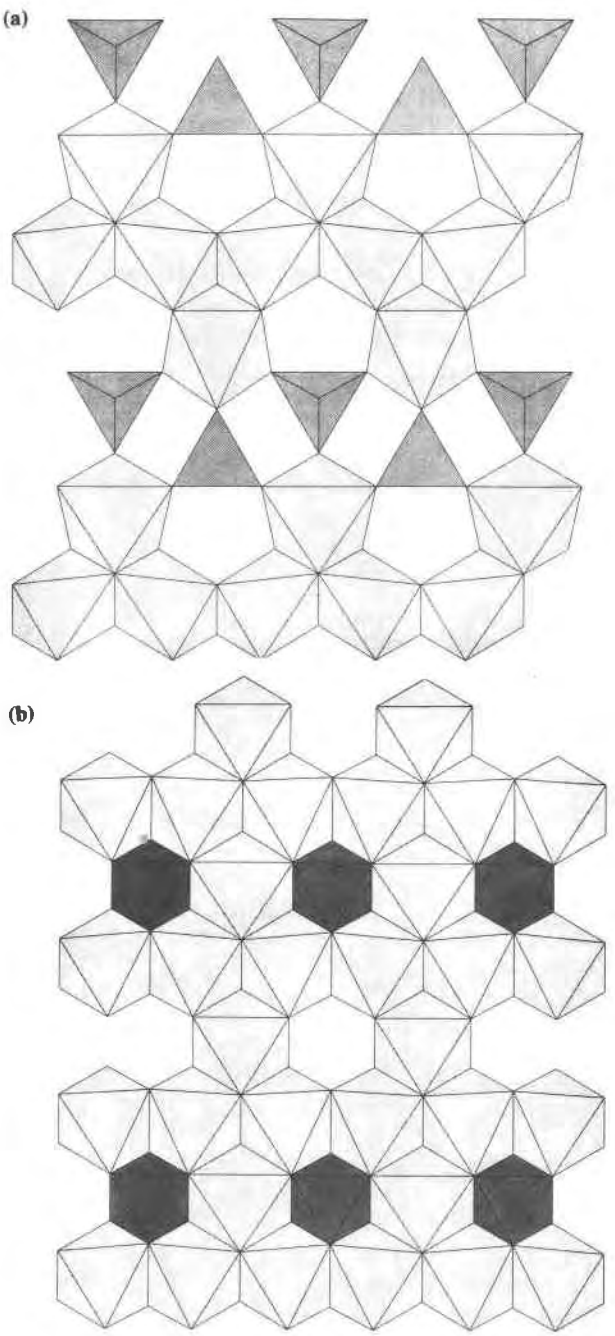

Fig. 1. Crystal structure of the two types of (010) layers found in phase AnhB, $Mg_{14}Si_5O_{24}$. **(a)** The olivine-like layer with tetrahedral Si and octahedral Mg. **(b)** The rock-salt layer with Mg and Si octahedra. The latter are indicated by the darker shading.

Discussion of structures

As noted above, the structures of these two phases are related. Parallel to b in each structure there is a stack of six layers of two types (Figs. 1, 2). One of these (010) layers (Figs. 1a, 2a) contains both Mg octahedra and Si tetrahedra in arrangements that have the stoichiometry,

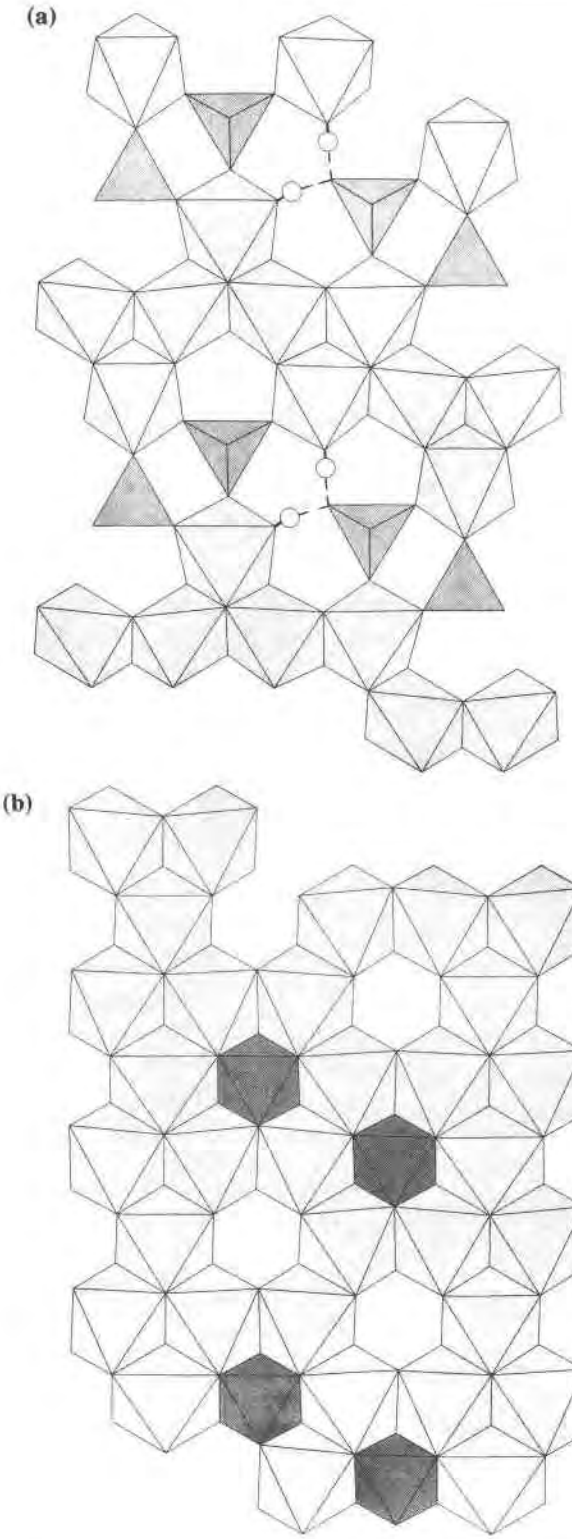

Fig. 2. Crystal structure of the two types of (010) layers found in phase B, $Mg_{12}Si_4O_{19}(OH)_2$. (a) The humite-like layer with tetrahedral Si and octahedral Mg. H atoms are marked with circles and short O-H bonds by solid lines, with the longer O-H bonds indicated by dashed lines. (b) The rock-salt layer with Mg and Si octahedra. The latter are indicated by darker shading.

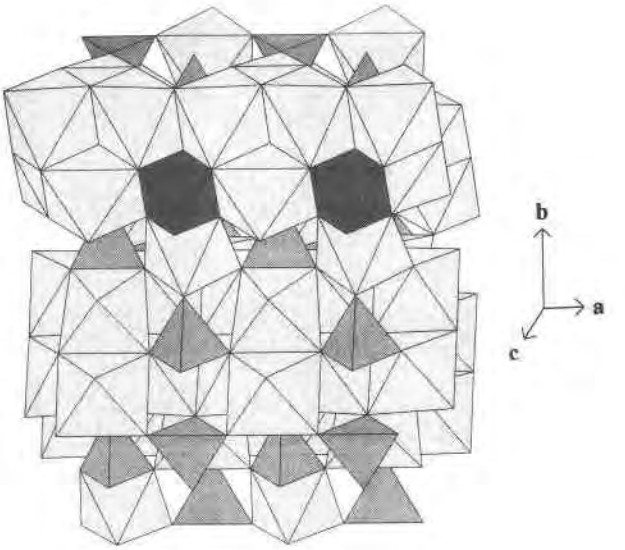

Fig. 3. The three dimensional structure of phase AnhB showing the cross linkages.

but not necessarily the topology, of the members of the olivine-humite series. The other layer (Figs. 1b, 2b) contains only octahedral cations, both Mg and Si, and may be described as a defect rock-salt layer, where the defects are vacancies and Si substituting for Mg, which is denoted by the small circles in the octahedra. There are two of the olivine-humite units per rock-salt layer in each of the structures. Figures 3 and 4 show the layer stacking and some of the interlayer linkages for phase AnhB and B,

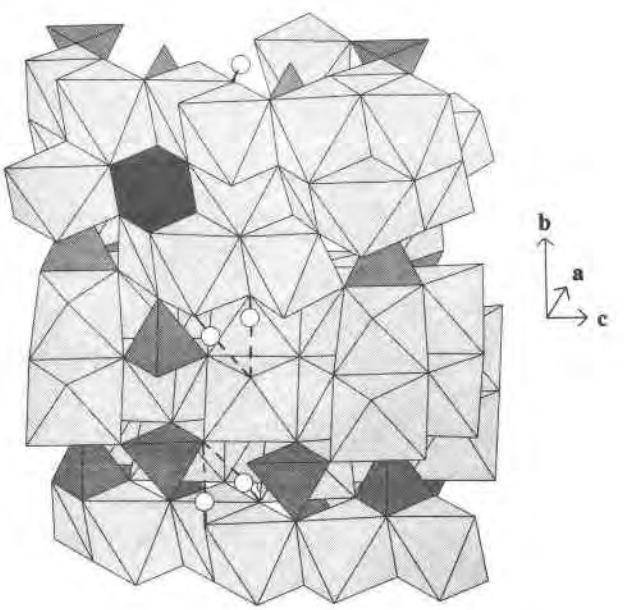

Fig. 4. The three dimensional structure of phase B showing the relative positions of the H atoms, which are indicated by small circles.

TABLE 5. Selected bond distances (Å) and angles (°) for phase AnhB

M-O	Distance	O-O	Distance	O-M-O
Si1-O2[2]*	1.818(2)	O2-O8[4]	2.562(2)	90.2(1)[4]
Si1-O8[4]	1.797(1)	O2-O8[4]	2.551(2)	89.8(1)[4]
mean	1.804	O8-O8[2]	2.519(3)	88.9(1)[2]
		O8-O8[2]	2.566(2)	91.1(1)[2]
Si2-O5	1.608(2)	O5-O6	2.732(3)	114.7(1)
Si2-O6	1.637(2)	O5-O9[2]	2.747(2)	116.2(1)[2]
Si2-O9[2]	1.627(1)	O6-O9[2]	2.541(2)	102.2(1)[2]
mean	1.625	O9-O9	2.552(2)	103.3(1)
Si3-O1	1.654(2)	O1-O3	2.710(3)	109.9(1)
Si3-O3	1.656(2)	O1-O7[2]	2.701(2)	109.2(1)[2]
Si3-O7[2]	1.659(1)	O3-O7[2]	2.688(2)	108.4(1)[2]
mean	1.657	O7-O7	2.747(3)	111.8(1)
Mg1-O5[2]	2.008(2)	O5-O7[4]	2.946(3)	90.4(1)[4]
Mg1-O7[4]	2.142(1)	O5-O7[4]	2.928(3)	89.6(1)[4]
mean	2.097	O7-O7[2]	3.119(3)	93.4(1)[2]
		O7-O7[2]	2.939(3)	86.6(1)[2]
Mg2-O4	2.224(2)	O4-O7[2]	2.953(2)	86.0(1)[2]
Mg2-O6	1.976(2)	O4-O9[2]	2.906(2)	84.8(1)[2]
Mg2-O7[2]	2.099(1)	O6-O7[2]	2.876(2)	89.7(1)[2]
Mg2-O9[2]	2.081(1)	O6-O9[2]	3.116(2)	100.3(1)[2]
mean	2.093	O7-O7	3.119(2)	95.9(1)
		O7-O9[2]	3.047(2)	93.5(1)[2]
		O9-O9	2.553(2)	75.6(1)
Mg3-O4[2]	2.112(2)	O4-O8[4]	2.995(3)	90.3(1)[4]
Mg3-O8[4]	2.109(1)	O4-O8[4]	2.978(3)	89.7(1)[4]
mean	2.110	O8-O8[2]	2.566(2)	75.0(1)[2]
		O8-O8[2]	3.348(3)	105.0(1)[2]
Mg4-O1	2.108(1)	O1-O2	3.054(2)	94.3(1)
Mg4-O2	2.056(1)	O1-O5	2.943(2)	90.6(1)
Mg4-O4	2.095(1)	O1-O7	2.914(2)	88.4(1)
Mg4-O5	2.030(1)	O1-O8	3.018(2)	91.6(1)
Mg4-O7	2.072(1)	O2-O4	2.949(2)	90.5(1)
Mg4-O8	2.099(1)	O2-O7	3.092(2)	96.9(1)
mean	2.077	O2-O8	2.564(2)	76.1(2)
		O4-O5	2.785(2)	84.8(1)
		O4-O7	2.953(2)	90.2(1)
		O4-O8	2.978(2)	90.4(1)
		O5-O7	2.928(2)	91.1(1)
		O5-O8	3.067(2)	95.9(1)
Mg5-O1	2.112(2)	O1-O8[2]	3.018(2)	88.9(1)[2]
Mg5-O3	2.112(2)	O1-O9[2]	2.877(2)	88.3(1)[2]
Mg5-O8[2]	2.192(1)	O3-O8[2]	2.994(2)	88.0(1)[2]
Mg5-O9[2]	2.012(1)	O3-O9[2]	3.014(2)	93.8(1)[2]
mean	2.106	O8-O8	2.520(2)	70.1(1)
		O8-O9[2]	2.965(2)	89.5(1)[2]
		O9-O9	3.315(3)	110.8(1)
Mg6-O2	2.061(1)	O2-O3	2.998(2)	92.5(1)
Mg6-O3	2.088(1)	O2-O4	2.949(2)	89.7(1)
Mg6-O4	2.119(1)	O2-O8	2.553(2)	76.0(1)
Mg6-O6	2.043(1)	O2-O9	3.282(3)	102.8(1)
Mg6-O8	2.081(1)	O3-O6	2.952(2)	91.2(1)
Mg6-O9	2.135(1)	O3-O8	2.994(2)	91.7(1)
mean	2.088	O3-O9	3.020(2)	91.2(1)
		O4-O6	2.857(2)	86.6(1)
		O4-O8	2.995(2)	90.9(1)
		O4-O9	2.906(2)	86.1(1)
		O6-O8	3.297(3)	106.1(1)
		O6-O9	2.542(2)	74.9(1)

* Numbers in square brackets indicate the multiplicity of the bond or angle.

TABLE 6. Selected bond distances (Å) and angles (°) for phase B

M-O	Distance	O-O	Distance	O-M-O
Si1-O12	1.795(3)	O12-O13	2.541(3)	90.2(1)
Si1-O13	1.797(3)	O12-O15	2.584(3)	88.9(1)
Si1-O14	1.787(3)	O12-O16	2.551(3)	90.4(1)
Si1-O15	1.897(3)	O12-O17	2.545(3)	90.3(1)
Si1-O16	1.804(3)	O13-O14	2.524(3)	89.7(1)
Si1-O17	1.800(3)	O13-O15	2.593(3)	89.2(1)
mean	1.813	O13-O16	2.768(3)	91.1(1)
		O14-O15	2.619(3)	90.7(1)
		O14-O16	2.535(3)	90.0(1)
		O14-O17	2.528(3)	89.8(1)
		O15-O17	2.602(3)	89.5(1)
		O16-O17	2.550(3)	90.2(1)
Si2-O9	1.631(2)	O9-O10	2.535(3)	102.5(1)
Si2-O10	1.624(3)	O9-O1	2.736(3)	115.1(1)
Si2-O1	1.614(3)	O9-O18	2.539(3)	102.8(1)
Si2-O18	1.621(3)	O10-O1	2.739(3)	115.7(1)
mean	1.623	O10-O18	2.521(3)	102.1(1)
		O1-O18	2.750(3)	116.6(1)
Si3-O5	1.651(3)	O5-O6	2.679(3)	107.8(1)
Si3-O6	1.666(3)	O5-O7	2.708(3)	109.9(1)
Si3-O7	1.661(3)	O5-O8	2.683(3)	108.8(1)
Si3-O8	1.652(3)	O6-O7	2.730(3)	110.4(1)
mean	1.658	O6-O8	2.737(3)	111.4(1)
		O7-O8	2.684(3)	108.5(1)
Si4-O19	1.644(3)	O19-O2	2.713(3)	110.4(1)
Si4-O2	1.665(3)	O19-O3	2.666(3)	108.3(1)
Si4-O3	1.646(3)	O19-O4	2.696(3)	109.8(1)
Si4-O4	1.656(3)	O2-O3	2.683(3)	108.5(1)
mean	1.653	O2-O4	2.728(3)	110.8(1)
		O3-O4	2.685(3)	109.0(1)
Mg1-O2[2]	2.096(2)	O2-O6[2]	3.084(3)	93.5(1)[2]
Mg1-O6[2]	2.144(2)	O2-O6[2]	2.903(3)	86.5(1)[2]
Mg1-O1[2]	2.017(2)	O2-O1[2]	2.921(3)	90.6(1)[2]
mean	2.086	O2-O1[2]	2.891(3)	89.4(1)[2]
		O6-O1[2]	2.935(3)	89.8(1)[2]
		O6-O1[2]	2.944(3)	90.2(1)[2]
Mg2-O2	2.086(3)	O2-O6	3.084(3)	95.5(1)
Mg2-O6	2.085(3)	O2-O9	2.865(3)	89.7(1)
Mg2-O9	1.980(3)	O2-O10	3.038(3)	94.1(1)
Mg2-O10	2.068(3)	O2-O11	2.950(3)	85.8(1)
Mg2-O11	2.251(3)	O6-O9	2.877(3)	90.1(1)
Mg2-O18	2.075(3)	O6-O11	2.979(3)	86.8(1)
mean	2.091	O6-O18	3.030(3)	93.7(1)
		O9-O10	3.105(3)	100.3(1)
		O9-O18	3.125(3)	101.0(1)
		O10-O11	2.879(3)	83.6(1)
		O10-O18	2.521(3)	75.1(1)
		O11-O18	2.893(3)	84.0(1)
Mg3-O11[2]	2.111(2)	O11-O12[2]	3.006(3)	90.2(1)[2]
Mg3-O12[2]	2.139(2)	O11-O12[2]	2.998(3)	89.8(1)[2]
Mg3-O16[2]	2.138(2)	O11-O16[2]	2.985(3)	89.4(1)[2]
mean	2.129	O11-O16[2]	3.015(3)	90.6(1)[2]
		O12-O16[2]	2.551(3)	73.4(1)[2]
		O12-O16[2]	3.426(3)	106.6(1)[2]
Mg4-O2	2.085(3)	O2-O7	2.965(3)	90.4(1)
Mg4-O7	2.100(3)	O2-O11	2.950(3)	89.2(1)
Mg4-O11	2.123(3)	O2-O13	3.189(3)	99.8(1)
Mg4-O13	2.088(3)	O2-O1	2.891(3)	88.8(1)
Mg4-O16	2.117(3)	O7-O13	3.054(3)	93.8(1)
Mg4-O1	2.049(3)	O7-O16	3.011(3)	91.3(1)
mean	2.094	O7-O1	2.965(3)	91.4(1)
		O11-O13	3.021(3)	91.8(1)
		O11-O16	2.985(3)	89.6(1)
		O11-O1	2.764(3)	83.1(1)
		O13-O16	2.568(3)	75.3(1)
		O16-O1	3.091(3)	95.9(1)
Mg5-O4	2.073(3)	O4-O8	2.938(3)	90.8(1)
Mg5-O8	2.061(3)	O4-O14	3.124(3)	98.5(1)
Mg5-O14	2.058(3)	O4-O15	3.004(3)	90.7(1)
Mg5-O15	2.141(3)	O4-O17	2.998(3)	92.8(1)
Mg5-O15	2.156(3)	O8-O14	2.989(3)	93.2(1)
Mg5-O17	2.071(3)	O8-O15	3.003(3)	91.4(1)
mean	2.093	O8-O17	3.109(3)	97.7(1)
		O14-O15	2.619(3)	77.3(1)
		O14-O15	3.047(3)	92.7(1)

respectively. Although the previous discussion described the structures in terms of these layers, there is as much linking between the layers as within; therefore, the structures are clearly three-dimensional. Selected bond distances and angles for phases AnhB and B are listed in Tables 5 and 6, respectively.

The octahedrally coordinated Si atoms in these structures have a special environment. Each octahedron shares all 12 edges with neighboring MgO_6 octahedra, and is,

TABLE 6—*Continued*

M-O	Distance	O-O	Distance	O-M-O
		O15-O15	2.972(3)	87.7(1)
		O15-O17	3.003(3)	91.0(1)
		O15-O17	2.602(3)	76.0(1)
Mg6-O19	2.094(3)	O19-O19	3.182(3)	98.8(1)
Mg6-O19	2.103(3)	O19-O7	3.077(3)	93.5(1)
Mg6-O7	2.134(3)	O19-O7	2.846(3)	84.5(1)
Mg6-O8	2.131(3)	O19-O8	2.886(3)	86.3(1)
Mg6-O13	2.125(3)	O19-O8	3.098(3)	94.1(1)
Mg6-O14	2.102(3)	O19-O13	3.066(3)	93.1(1)
mean	2.115	O19-O14	3.088(3)	95.0(1)
		O7-O13	3.054(3)	91.8(1)
		O7-O14	3.031(3)	91.5(1)
		O8-O13	2.971(3)	88.7(1)
		O8-O14	2.989(3)	90.0(1)
		O13-O14	2.524(3)	73.5(1)
Mg7-O4	2.073(3)	O4-O6	2.899(3)	88.4(1)
Mg7-O6	2.090(3)	O4-O12	2.981(3)	90.4(1)
Mg7-O11	2.086(3)	O4-O17	2.998(3)	92.6(1)
Mg7-O12	2.131(3)	O4-O1	2.930(3)	90.8(1)
Mg7-O17	2.079(3)	O6-O11	2.979(3)	91.1(1)
Mg7-O1	2.047(3)	O6-O17	3.145(3)	98.1(1)
mean	2.085	O6-O1	2.944(3)	90.9(1)
		O11-O12	2.998(3)	90.8(1)
		O11-O17	3.009(3)	92.6(1)
		O11-O1	2.764(3)	84.0(1)
		O12-O17	2.545(3)	74.5(1)
		O12-O1	3.114(3)	96.6(1)
Mg8-O3	2.060(3)	O3-O9	2.934(3)	90.7(1)
Mg8-O9	2.068(3)	O3-O10	3.011(3)	92.5(1)
Mg8-O10	2.113(3)	O3-O12	2.969(3)	91.2(1)
Mg8-O11	2.131(3)	O3-O13	2.978(3)	92.3(1)
Mg8-O12	2.097(3)	O9-O10	2.535(3)	74.7(1)
Mg8-O13	2.074(3)	O9-O11	2.837(3)	85.1(1)
mean	2.091	O9-O12	3.284(3)	104.3(1)
		O10-O11	2.879(3)	85.5(1)
		O10-O13	3.332(3)	105.6(1)
		O11-O12	3.006(3)	90.7(1)
		O11-O13	3.021(3)	91.9(1)
		O12-O13	2.541(3)	75.2(1)
Mg9-O5	2.079(3)	O5-O14	3.021(3)	92.5(1)
Mg9-O14	2.104(3)	O5-O17	2.998(3)	91.4(1)
Mg9-O15	2.264(3)	O5-O20	2.939(3)	91.4(1)
Mg9-O17	2.115(3)	O5-O21	3.017(3)	95.3(1)
Mg9-O20	2.029(3)	O14-O15	3.047(3)	88.4(1)
Mg9-O21	2.008(3)	O14-O17	2.528(3)	73.7(1)
mean	2.100	O14-O21	3.168(3)	100.9(1)
		O15-O17	3.003(3)	86.6(1)
		O15-O20	2.964(3)	87.2(1)
		O15-O21	2.942(3)	86.9(1)
		O17-O20	3.091(3)	96.6(1)
		O20-O21	2.806(3)	88.2(1)
Mg10-O5	2.087(3)	O5-O14	3.020(3)	87.7(1)
Mg10-O7	2.122(3)	O5-O16	2.953(3)	88.6(1)
Mg10-O14	2.273(3)	O5-O20	2.944(3)	92.3(1)
Mg10-O16	2.146(3)	O5-O18	3.018(3)	95.8(1)
Mg10-O20	2.000(3)	O7-O14	3.031(3)	87.2(1)
Mg10-O18	1.984(3)	O7-O16	3.011(3)	89.9(1)
mean	2.102	O7-O20	2.852(3)	87.7(1)
		O7-O18	2.881(3)	89.2(1)
		O14-O16	2.535(3)	70.0(1)
		O14-O20	3.084(3)	92.3(1)
		O16-O18	2.983(3)	92.5(1)
		O20-O18	3.157(3)	105.0(1)
Mg11-O3	2.132(3)	O3-O10	3.050(3)	96.1(1)
Mg11-O4	2.121(3)	O3-O12	2.969(3)	89.6(1)
Mg11-O10	1.972(3)	O3-O15	3.003(3)	87.1(1)
Mg11-O12	2.084(3)	O3-O21	2.844(3)	87.5(1)
Mg11-O15	2.231(3)	O4-O10	2.880(3)	89.5(1)
Mg11-O21	1.980(3)	O4-O12	2.981(3)	90.4(1)
mean	2.087	O4-O15	3.004(3)	87.4(1)
		O4-O21	2.918(3)	90.8(1)
		O10-O12	2.970(3)	94.3(1)
		O10-O21	3.103(3)	103.7(1)
		O12-O15	2.584(3)	73.6(1)
		O15-O21	2.942(3)	88.6(1)

TABLE 6—*Continued*

M-O	Distance	O-O	Distance	O-M-O
Mg12-O5	2.066(3)	O5-O9	2.931(3)	90.8(1)
Mg12-O9	2.054(3)	O5-O16	2.953(3)	90.9(1)
Mg12-O11	2.133(3)	O5-O17	2.998(3)	92.6(1)
Mg12-O16	2.083(3)	O5-O18	3.003(3)	91.8(1)
Mg12-O17	2.085(3)	O9-O11	2.837(3)	85.4(1)
Mg12-O18	2.121(3)	O9-O16	3.286(3)	105.3(1)
mean	2.090	O9-O18	2.539(3)	75.0(1)
		O11-O16	3.015(3)	91.5(1)
		O11-O17	3.009(3)	91.1(1)
		O11-O18	2.893(3)	85.8(1)
		O16-O17	2.550(3)	75.5(1)
		O17-O18	3.313(3)	104.0(1)
Mg13-O3	2.134(3)	O3-O13	2.978(3)	88.9(1)
Mg13-O8	2.127(3)	O3-O15	3.003(3)	88.3(1)
Mg13-O13	2.122(3)	O3-O20	2.924(3)	90.6(1)
Mg13-O15	2.183(3)	O3-O21	2.949(3)	91.9(1)
Mg13-O20	1.981(3)	O8-O13	2.971(3)	88.8(1)
Mg13-O21	1.973(3)	O8-O15	3.003(3)	88.5(1)
mean	2.087	O8-O20	2.924(3)	90.8(1)
		O8-O21	2.921(3)	90.9(1)
		O13-O15	2.593(3)	74.1(1)
		O13-O21	2.989(3)	93.8(1)
		O15-O20	2.964(3)	90.7(1)
		O20-O21	3.055(3)	101.3(1)
H1-O20	0.93(6)	O19-O20	2.882(3)	172(5)
H1-O19	1.96(6)			
H2-O21	0.82(5)	O19-O21	2.852(4)	173(5)
H2-O19	2.03(5)			
H1-H2	1.93(6)			

therefore, at the center of a 13 cation cluster. The large amount of edge sharing among the octahedra is responsible, in part, for the high density of these phases. There is, however, limited edge sharing between octahedra and tetrahedra. In phase AnhB, one of the crystallographically distinct tetrahedrally coordinated Si atoms shares only corners with the octahedra, a topology similar to that of spinel. The other tetrahedron shares two edges with Mg octahedra as contrasted to the three shared edges in olivine. In phase B, two of the distinct tetrahedra share only corners with octahedra. The third tetrahedron shares edges with the octahedra. The SiO_6 octahedra are regular with quadratic elongation and angle variance values (Robinson et al., 1971) of 1.000 and 0.5 for phase AnhB, and 1.001 and 0.4 for phase B. By way of contrast, the MgO_6 octahedra have distortions that range up to 1.025 for the quadratic elongation and 101.0 for the angular variance.

All H bonding in phase B occurs within the humite-like layer, rather than between layers. The resulting H bonding tends to increase, rather than decrease the density of the structure. In Figures 2 and 4, the short O-H bonds (~1 Å) are indicated by a solid bar. Dashed lines represent the longer O-H bonds of ~2 Å. Note also that the H-H separation is only 1.9 Å. Each of the donor O atoms (O20 and O21) has a distorted tetrahedral coordination consisting of three Mg atoms and one H atom. The receptor O atom (O19) is coordinated by two Mg atoms, one Si atom, and two H atoms at long distances.

The final conclusion to be reached is that high-pressure materials do not always have simple structures. For materials as complicated as found in this study, it will be extremely difficult, if not impossible, to deduce atomic

arrangements from quenched powders. High-quality single crystals, such as obtained from the new generation of large-volume, high-pressure devices, are essential.

Acknowledgments

We wish to thank T. Gasparik and J. Ko of the Stony Brook High-Pressure Laboratory for providing the crystals used in this study and D. Veblen of Johns Hopkins University for TEM investigation of the phase B sample. The X-ray laboratory facilities are supported in part by the National Science Foundation Grants EAR86-18602 (C.T.P.), EAR89-16709 (R.M.H. and L.W.F.) and EAR87-08192 (R.M.H. and R.J. Hemley) and by the Carnegie Institution of Washington. We also thank Josef Zemann for his thoughtful criticisms, which helped us improve this report.

References cited

Akaogi, M., and Akimoto, S. (1980) High-pressure stability of a dense hydrous magnesian silicate $Mg_{23}Si_8O_{42}H_6$ and some geophysical implications. Journal of Geophysical Research, 85, 6944–6948.

Brown, I.D. (1981) The bond-valence method: An empirical approach to chemical structure and bonding. In M. O'Keeffe and A. Navrotsky, Eds., Structure and bonding in crystals, vol. II, p. 1–30. Academic Press, New York.

Burnham, C.W. (1966) Computation of absorption corrections, and the significance of end effects. American Mineralogist, 51, 159–167.

Deer, W.A., Howie, R.A., and Zussman, J. (1962) In Rock-forming minerals, vol. 3: Sheet silicates. Wiley, New York.

——— (1963) In Rock-forming minerals, vol. 2: Chain silicates. Wiley, New York.

Downs, J.W. (1989) Possible sites for protonation in β-Mg_2SiO_4 from an experimentally derived electrostatic potential. American Mineralogist, 74, 1124–1129.

Finger, L.W., and Prewitt, C.T. (1989) Predicted compositions for high-density hydrous magnesium silicates. Geophysical Research Letters, 16, 1395–1397.

Finger, L.W., and Prince, E. (1975) A system of Fortran IV computer programs for crystal structure computations. NBS Technical Note 854.

Finger, L.W., Ko, J., Hazen, R.M., Gasparik, T., Hemley, R.J., Prewitt, C.T., and Weidner, D.J. (1989) Crystal chemistry of phase B and an anhydrous analogue: Implications for water storage in the upper mantle. Nature, 341, 140–142.

Gasparik, T. (1990) Phase relations in the transition zone. Journal Geophysical Research, 95, 15751–15769.

Gilmore, C.J. (1984) MITHRIL—an integrated direct-methods computer program. Journal of Applied Crystallography, 17, 42–46.

Herzberg, C., and Gasparik, T. (1989) Melting experiments on chondrite at high pressures: Stability of anhydrous phase B. Eos, 70, 484.

Horiuchi, H., Morimoto, N., Yamamato, K., and Akimoto, S. (1979) Crystal structure of $2Mg_2SiO_4 \cdot 3Mg(OH)_2$, a new high-pressure structure type. American Mineralogist, 64, 593–598.

Kanzaki, M. (1989) High pressure phase relations in the system MgO-SiO_2-H_2O. Eos, 70, 508.

McGetchin, T.R., Silver, L.T., and Chodos, A.A. (1970) Titanoclinohumite: A possible mineralogical site for water in the upper mantle. Journal of Geophysical Research, 75, 255–259.

Ribbe, P.H. (1980) The humite series and Mn-analogs. In Mineralogical Society of America Reviews in Mineralogy, 5, 231–274.

Rice, S.B., Benimoff, A.I., and Sclar, C.B. (1989) "3.65 Å phase" in system MgO-SiO_2-H_2O at pressures greater than 90 kbars: Crystallochemical implications for mantle phases. Abstracts of International Geological Congress, Washington DC Meeting, 2, 694.

Ringwood, A.E., and Major, A. (1967) High-pressure reconnaissance investigations in the system Mg_2SiO_4-MgO-H_2O. Earth and Planetary Science Letters, 2, 130–133.

Robinson, K., Gibbs, G.V., and Ribbe, P.H. (1971) Quadratic elongation: A quantitative measure of distortion in coordination polyhedra. Science, 172, 567–570.

Sclar, C.B., and Carrison, L.C. (1966) High-pressure reactions and shear strength of serpentinized dunite. Science, 153, 1285–1286.

Sclar, C.B., Carrison, L.C., and Schwartz, C.M. (1965) High-pressure synthesis and stability of a new hydronium-bearing layer silicate in the system MgO-SiO_2-H_2O. Transactions American Geophysical Union, 48, 184.

Smyth, J.R. (1987) β-Mg_2SiO_4: A potential host for water in the mantle? American Mineralogist, 72, 1051–1055.

Von Dreele, R.B., Bless, P.W., Kostiner, E., and Hughes, R.E. (1970) The crystal structure of magnesiium germanate: A reformulation of Mg_4GeO_6 as $Mg_{28}Ge_{10}O_{48}$. Journal of Solid State Chemistry, 2, 612–618.

Yamamoto, K., and Akimoto, S. (1977) The system MgO-SiO_2-H_2O at high pressures and temperatures—stability field for hydroxyl-chondrodite, hydroxyl-clinohumite and 10 Å-phase. American Journal of Science, 277, 288–312.

Manuscript received March 20, 1990
Manuscript accepted November 10, 1990